Clays and Clay Minerals, Vol. 55, No. 6, 618–634, 2007.

CLAY MINERAL FORMATION DURING PODZOLIZATION IN AN ALPINE ENVIRONMENT OF THE TATRA MOUNTAINS, POLAND

MICHAŁ SKIBA*

Institute of Geological Sciences, Jagiellonian University, ul. Oleandry 2a, 30-063 Kraków, Poland

Abstract—The processes of clay mineral formation were studied in seven podzol profiles developed on granitic regoliths in the Polish part of the Tatra Mountains. The selected profiles have similar parent material and macroscopically represent different stages of soil development (from initial to advanced). Bulk soil material (<2 mm fraction) and separated clay fractions (<2 μm) were studied using a petrographic microscope, X-ray diffraction, Fourier transform infrared spectroscopy, and scanning electron microscopy-energy-dispersive spectrometry methods. The mineral compositions of the bulk soil samples are more or less the same (quartz, feldspars, mica and minor amounts of other phyllosilicates). The clay fractions are composed of mica and mixed-layer minerals which contain hydrated interlayers of vermiculitic and/or smectitic type, and kaolinite. Smaller amounts of chlorite, feldspars and quartz were also identified. Chlorite is present almost exclusively (except for one profile) in lower soil horizons (C, B/C, B). The amount of minerals with hydrated interlayers increases up the profiles. Kaolinite is present in all the samples except for the lowermost soil horizons (C) of two of the profiles. In some of the B horizons, the formation of hydroxy interlayers within hydrated interlayers is observed. The main processes of clay mineral formation recognized in the soils studied are: inheritance from the parent rocks; crystallization of kaolinite from soil solutions; the formation of dioctahedral vermiculite at the expense of inherited dioctahedral mica, and the formation of dioctahedral smectite at the expense of vermiculite. The recognized sequence of transformation is as follows: M → R0 M-V (12 Å or 14 Å) → R0 M-12 Å V → R1 M-12 Å V → 12 Å V → V-S → S. Observed formation of hydroxy interlayers seems to be pH dependent, starting when the pH ⩾4.4. The process of dissolution of primary silicates occurring simultaneously with the transformation is also documented.

Key Words—Hydroxy interlayering, Kaolinite, Podzols, Smectite, Vermiculite, Weathering.

INTRODUCTION

Podzolization is a soil-forming process involving natural acidification and weathering of parent material in upper mineral soil horizons, transport of the weathering products down the profile, and precipitation of new phases (*e.g.* Prusinkiewicz, 1994; Lundström *et al.*, 2000). The acidification is caused by organic acids (humic acids, fulvic acids as well as low molecular weight organic acids) which are produced in organic soil horizons by plants, bacteria and fungi and the processes of organic matter oxidation. The organic acids cause destruction of primary minerals as well as playing an important role in the transport of dissolved species due to the formation of metallo-organic complexes (*e.g.* Konecka-Betley *et al.*, 1999; Lundström *et al.*, 2000). It is widely accepted that podzolization is favored by certain mineral compositions and the texture of the parent rock, by the presence of acidophilic plants, and by climatic conditions with high precipitation (Prusinkiewicz, 1994; Lundström *et al.*, 2000, and literature cited therein).

Characteristic soil horizons can be distinguished in well developed podzol profiles including the uppermost organic horizons (OFH), the upper light-colored mineral horizon called the albic horizon (E), lower dark-colored mineral spodic horizons (Bhf and Bs), and parent material which exhibits a different degree of alteration: Bs/C – intermediate horizon, C – parent material, R – solid bedrock (Prusinkiewicz, 1994; Lundström *et al.*, 2000).

The destruction of parent minerals and mobilization of weathering products dominate in the albic horizon, whereas the precipitation of new phases takes place in the spodic horizon. According to the criteria given by the *World Reference Base for Soil Resources* (Bednarek *et al.*, 2003), the spodic horizon is the diagnostic horizon for podzols.

Numerous papers concerning the mineral composition of podzols have been published (*e.g.* Gorbunov *et al.*, 1963; Kodama and Brydon, 1966; Bain, 1977; Wilson *et al.*, 1984; Bain *et al.*, 1990; Righi *et al.*, 1993; Righi *et al.*, 1997a; Righi *et al.*, 1999; Bain and Fraser, 1994; Gustafsson *et al.*, 1995; McDaniels *et al.*, 1995; Lång and Stevens, 1996; Righi and Elsass, 1996; Carnicelli *et al.*, 1997; Weber *et al.*, 1998; Gillot *et al.*, 2000; Melkerud *et al.*, 2000; Gillot *et al.*, 2001; Egli *et al.*, 2001; Mirabella *et al.*, 2002; Egli *et al.*, 2002; Lin *et al.*, 2002; Egli *et al.*, 2003). The main processes recognized are the transformation of primary micas or chlorite (or both) into dioctahedral vermiculite, and the formation of dioctahedral smectite (Fe-rich beidellite) at the expense of

* E-mail address of corresponding author:
skiba@geos.ing.uj.edu.pl
DOI: 10.1346/CCMN.2007.0550609

vermiculite (*e.g.* Bain *et al.*, 1990; Carnicelli *et al.*, 1997; Righi *et al.*, 1997a). Transformation of dioctahedral mica directly into smectite was also suggested by Righi *et al.* (1999). Dioctahedral smectite in podzols is thought to be the end-product of mica transformation although its neoformation was documented in soils developed on volcanic ash deposits devoid of mica (McDaniels *et al.*, 1995). Allophane and imogolite formation in podzols was described in detail by many authors (*e.g.* Farmer *et al.*, 1980; Gustafsson *et al.*, 1995). The possibility of kaolinite crystallization was suggested by Gorbunov *et al.* (1963). It is also widely accepted that hydroxy-Al interlayering of vermiculite and smectite is common in podzols and it seems to be pH dependent (Bain *et al.*, 1990).

Despite the abundance of papers published, several problems with podzol mineralogy remain unsolved: the origin of kaolinite which is not widely discussed in the literature (Skiba, 2001, and literature cited therein), and the transformation sequence leading to the formation of stable smectite (Fe-rich beidellite?) at the expense of primary layer silicates (Środoń, 1999, and literature cited therein). According to the author's knowledge, data concerning feldspar weathering in a podzol environment are also rare (*e.g.* van Breemen *et al.*, 2000; Hoffland *et al.*, 2002). These issues are addressed in the present study of the podzols from the Tatra Mountains.

The chemical properties of Tatra podzols have been described in detail and their origin discussed (*e.g.* Skiba, 1977). A few mineralogical papers regarding Tatra podzols are available (*i.e.* Kubisz and Oleksynowa, 1972; Oleksynowa and Skiba, 1976; Skiba, 2001). Numerous studies of the mineralogy of the Tatra crystalline rocks, the parent rocks for the podzols, have been carried out (*e.g.* Michalik and Uchman, 1998 and literature cited therein). The data concerning the Tatra natural environment are also abundant (*e.g.* Skiba, 1998). Thus the processes which control the evolution of mineral composition of podzols can be well constrained for the Tatra samples.

MATERIALS AND METHODS

Site and material description

The Tatra Mountains are located in Central Europe within the inner part of the Carpathians. The elevations range from 900 to 2600 m a.s.l. Like most alpine environments, the Tatras exhibit elevation-dependent zonation of vegetation and climate with the mean annual temperature ranging from +6ºC to −4ºC and the precipitation from 844 mm to 1991 mm (Niedźwiedź, 1992). Almost 30% of the area is covered by podzols which are developed mainly on crystalline rocks (Variscian granitoids and pre-Carboniferous metamorphic rocks) and on glacial tills composed of similar rocks.

The samples were collected from seven podzol profiles, developed under slightly different climatic conditions, and derived from similar parent rocks. The chosen profiles represent different stages of soil profile development (S. Skiba, pers. comm., 2001): from poorly developed with only a slight spodic horizon visible to advanced with well developed albic and spodic horizons. Most of the soils and their chemical properties were described in detail by Skiba and Skiba (2005). A simplified profile description is given in Table 1.

Sample preparation and XRD techniques

Bulk-soil material (<2 mm fractions) and clay-size fractions (<2 μm) were analyzed.

The bulk-soil samples were air dried and passed through a 2 mm steel sieve. A small amount (~5 g) of each sample (<2 mm fraction) was ground in an agate mortar. The ground samples were then side-loaded to obtain random powder mounts for XRD analysis.

Organic matter was removed from an aliquot of each sample using 15% hydrogen peroxide buffered with an acetic acid buffer (pH ~5). The free Fe oxides were removed from each sample according to the method of Mehra and Jackson (1960). Finally each sample was Na saturated and dialyzed. After the treatment, the clay fractions (<2 μm) were separated by centrifugation and air dried. Oriented samples on glass slides with a surface density of 5 mg/cm^2 clay were prepared by deposition of the clay fractions resuspended in distilled water. After the analyses of Na-saturated samples, two of the profiles (Profile 1: Dolina Suchej Wody Valley and Profile 6: Trzydniowiański Wierch Mountain) were selected for more detailed X-ray analysis employing random powder mounts prepared from the clay fractions as well as the analysis of the oriented mounts of the clay fractions in K-saturated and Mg-saturated form.

X-ray diffraction analyses were performed with the use of a Philips X'Pert diffractometer with vertical goniometer PW3020, equipped with a 1º divergence slit, 0.2 mm receiving slit, incident- and diffracted-beam Soller slits, 1º anti scatter slit, and a graphite diffracted-beam monochromator. CuKα radiation was used with an applied voltage of 40 kV and 30 mA current. The mounts were scanned from 2 to 64º2θ at a counting time of 1 s per 0.02º2θ step (random mounts of the bulk soil materials and oriented slides of <2 μm fractions in Na form) and 5 s per 0.02º step (random mounts of <2 μm fractions and oriented slides of <2 μm fractions in Mg and K form). The analyses of the oriented slides were performed in air-dry conditions, after ethylene-glycol vapor treatment, after glycerol saturation (for Mg-saturated samples only) and after 1 h heating at 200ºC, 330ºC and 550ºC sequentially. The XRD patterns were processed using the ClayLab computer program (Mystkowski, 1999). Simulations of XRD patterns of mixed-layer clay minerals were performed using the NEWMOD computer program (Reynolds, 1985).

Fourier transform infrared spectroscopy

All the clay fractions were analyzed using a Fourier transform infrared (FTIR) spectrometer FTS 135 Bio Rad.

https://doi.org/10.1346/CCMN.2007.0550609 Published online by Cambridge University Press

Table 1. Parent rocks and some specific properties of the soils investigated.

Soil depth (cm)	Soil horizon	>2 mm (vol.%)	pH (H_2O)	Parent rock description
Profile 1: Dolina Suchej Wody Valley, 1055 m a.s.l.				
0–7	OFH		4.4	
7–18	E	10	4.0	Cobbles rich sandy till derived from tonalites, K-feldspar-rich pegmatitic granites, and Triassic quartzites. Besides quartz and feldspars the granitoids contain muscovite, partly chloritized biotite, and a significant amount of feldspar-derived 'sericite'.
18–30	Bhf	30	4.4	
30–65	Bs	50	4.5	
65–100	Bs/C	60	4.8	
>100	C	60	5.0	
Profile 2: Czarny Staw Lake, 1640 m a.s.l.				
0–16	OE	20	3.5	Boulder-dominated till composed of tonalite and K-feldspar-rich pegmatitic granite boulders. Besides quartz, the granitoids contain muscovite, partly chloritized biotite and sericitized feldspars.
16–34	Bs/C	60	4.2	
>34	R			
Profile 3: Krzyżne Pass, 2130 m a.s.l.				
0–2	OFH		4.1	
2–6	A		3.9	
6–12	E	10	4.2	Weathered (arenitized) tonalities which contain quartz, muscovite, partly chloritized biotite and sericitized feldspars
12–20	Bhf	20	4.6	
20–35	Bs	40	4.8	
35–65	Bs/C	40	4.9	
>65	C	60	4.9	
Profile 4: Beskid Mountain, 1960 m a.s.l.				
0–12	OE	20	4.9	
12–20	Bhf	40	4.9	Weathered crystalline schists, which contain significant amounts of chlorite, quartz, sericitized feldspars, biotite and muscovite
20–30	Bs/C	70	5.1	
>30	R			
Profile 5: Dolina Jarząbcza Valley, 1200 m a.s.l.				
0–7	OFH		3.8	
7–12	E	30	3.5	Sandy till rich in cobbles of gneisses and muscovite, biotite and chlorite schists.
12–35	Bhf	40	4.3	
35–70	Bs/C	60	4.8	
>70	C	80	4.8	
Profile 6: Trzydniowiański Wierch Mountain, 1620 m a.s.l.				
0–10	OFH		4.2	
10–20	E	10	4.3	Scree containing angular clasts of leucogranites and gneisses. The rocks are made of quartz, partly sericitized feldspars, muscovite, biotite and chlorite.
20–45	Bhf	20	4.7	
45–60	Bs/C	60	5.0	
>60	R			
Profile 7: Trzydniowiański Wierch Mountain – the peak, 1750 m a.s.l.				
0–5	OFH		4.0	
5–10	E	20	4.0	Disintegrated (arenitized or sheared) leucogranites. Macroscopically the 'arenites' contain quartz, altered feldspars and muscovite.
10–30	Bhf	40	4.6	
30–70	Bs/C	70	5.1	
>70	C	80	5.1	

The spectra were recorded in the range 400 to 4000 cm^{-1} at a resolution of 1 cm^{-1}. The samples were prepared as pressed pellets after hand grinding (0.6 mg of clay with 300 mg of potassium bromide) in an agate mortar.

Microscopy observations

The samples from profile 1, Dolina Suchej Wody Valley, and Profile 3, Krzyżne Pass, were selected, based on the XRD and IR data, for detailed observation using petrographic and scanning electron microscopes (SEM). A field emission scanning electron microscope (FESEM) (Hitachi S-4700 equipped with a Vantage Noran EDS system) and a back scattered electrons detector (YAG BSE) were used. Natural surfaces of grains of >2 mm and polished thin-sections from the soil material were prepared by carbon coating for examination by SEM. Carbon-coated, oriented preparations of dispersed clay fractions were also prepared by evaporating a small amount of the diluted clay suspensions (~1.8 mg sample/20 cm^3 distilled water + a few drops of ammonia added for better dispersion) on polished carbon plates coated with gold.

https://doi.org/10.1346/CCMN.2007.0550609 Published online by Cambridge University Press

RESULTS

Mineral composition of the bulk-soil material

All the soils studied consisted mainly of quartz, K-feldspar and Na-plagioclase. Small amounts of layer silicates, mainly mica and chlorite, were also identified in the samples collected from the lower parts of the profiles (C, B/C) by the presence of their basal (near 14 Å, 10 Å, 7 Å) and *hkl* reflections (near 4.5 Å, 2.56 Å, 1.50 Å). Weak, broad reflections between 10 Å and 14 Å were observed for samples from the upper soil horizons (E, OE). They are interpreted to be due to mixed-layer clay minerals.

Operational definitions used during identification of clay minerals

Vermiculite was identified after Na exchange by its basal 001 reflection near 14 Å after ethylene glycol treatment. In air-dry conditions Na-vermiculite has its basal 001 reflection at 12.5 Å or 14 Å (Brindley and Brown, 1980), while after heating at 330ºC, the reflection moves to 10 Å. Two types of vermiculite have been distinguished in the studied samples. These are swelling and non-swelling vermiculite, referred to hereafter as 12.5 Å vermiculite and 14 Å vermiculite, respectively. After Mg saturation, air-dried vermiculite gives a basal 001 reflection near 14 Å, which does not shift after glycerol treatment.

Vermiculite with hydroxy interlayers was identified by its partial thermal stability, manifested by incomplete collapse of its basal 001 reflection after Na saturation and heating at 330ºC. The reflection shifts to 10 Å after heating at 550ºC.

The identification of kaolinite was performed in air-dry conditions based on the presence of its second-order 002 basal reflection near 3.58 Å The reflection does not shift after ethylene glycol treatment, but disappears after heating at 550ºC. The XRD identification of kaolinite was confirmed by the presence of an OH-stretching band near 3697 cm^{-1} in FTIR spectra.

Smectite was identified in air-dried Na-saturated mounts by the presence of a sharp basal 001 reflection near 12.5 Å, which shifts to ~17 Å after ethylene glycol treatment. The mineral displays an almost rational series of higher-order reflections. Following Mg saturation, the basal 001 reflection shifts to >17 Å after glycerol treatment.

Chlorite was identified by basal 001, 002, 003, 004 reflections near 14, 7, 4.72 and 3.52 Å, respectively, which do not change position or intensity after ethylene glycol treatment. The intensity of the 001 chlorite reflection increases and the intensities of the higher-order reflections decrease after heating at 550ºC.

Mica (illite-type mineral) was identified by the presence of basal reflections 001, 002, 003, 004, 005 near 10, 5, 3.33, 2.5 and 2.0 Å, respectively, which do not change intensity or position after any diagnostic tests.

Trioctahedral and dioctahedral species were distinguished in the XRD patterns of the random powder mounts by the presence of their 060 reflections near 1.54 Å and 1.49–1.51 Å, respectively. The presence of dioctahedral 2:1 species was also confirmed by the presence of an OH-stretching band near 3620 cm^{-1} in the FTIR spectra. Identification of trioctahedral minerals was difficult because of the potential overlap of 060 reflections with the quartz 211 peak. The occurrence of small amounts of trioctahedral minerals was indicated by the presence of Mg-OH or Fe-OH bending bands near 650 cm^{-1} in the FTIR spectra – according to the criterion given by Madejová (2003).

MINERAL COMPOSITION OF THE SEPARATED CLAY FRACTIONS

Profile 1, Dolina Suchej Wody Valley

The clay fraction separated from the C horizon contains mica, chlorite and mica-12.5 Å vermiculite mixed-layered minerals. A slight elevation of the background between 10 Å and 14 Å after heating at 550ºC may suggest the presence of chloritic interlayers in the mixed-layer minerals. Quartz and feldspars were also recognized.

In the fraction separated from the Bs/C horizon, besides mica, chlorite and mica-12.5 Å vermiculite, pure 14 Å vermiculite appears (Figure 1). Its presence is strongly indicated by the decrease in intensity of the 14 Å reflection after heating at 330ºC. The fraction contains also small amounts of kaolinite and non-clay minerals such as quartz and feldspars.

Mica and 14 Å vermiculite occur in the clay fractions from the Bs and Bhf horizons. There is also kaolinite, chlorite, quartz, feldspars and a mixed-layer mineral which contains swelling interlayers probably of vermiculitic type, although the significant decrease of the 10–14 Å reflection intensity after the glycol treatment may suggest an admixture of smectitic interlayers. Incomplete collapse to 10 Å after heating at 330ºC (Figure 2) indicates the presence of hydroxy interlayers in the vermiculite and/or mixed-layer mineral.

The clay fraction of the uppermost albic (E) horizon is dominated by mixed-layer minerals with large amounts of swelling interlayers of both vermiculitic and smectitic type. This fraction also contains kaolinite, mica, quartz and a small amount of feldspars. In the XRD pattern of air-dried Mg-saturated clay, the superstructure reflection near 24 Å can be seen, indicating the presence of a small amount of ordered (R = 1) mica-vermiculite (Figure 3).

The pattern of the Mg-saturated sample was modeled (Figure 3) using the NEWMOD program (Reynolds, 1985) and the best fit between calculated and measured XRD patterns was obtained for a mixture of dioctahedral vermiculite (N = 5) with vermiculite-smectite (R0, 70% smectite N = 3), illite (N = 10 and N = 3), kaolinite

https://doi.org/10.1346/CCMN.2007.0550609 Published online by Cambridge University Press

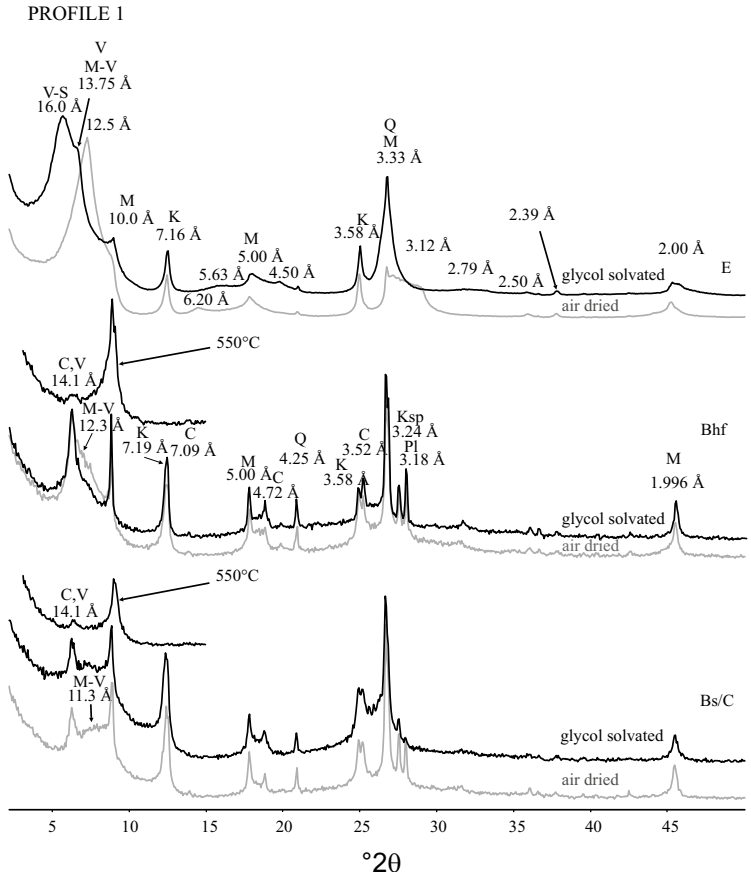

Figure 1. Profile 1: XRD patterns of the air-dried, EG-solvated, and heated at 550ºC oriented mounts of Na-saturated clay fractions. C – chlorite, Ksp – K-feldspars, Pl – plagioclase, M – mica, S – smectite, V – vermiculite, Q – quartz, K – kaolinite, Vhx – hydroxy-interlayered vermiculite. CuKα radiation.

(N = 29), illite-vermiculite mixed-layer mineral (R1, 50% vermiculite, N = 5) and illite-vermiculite mixed-layer mineral (R1, 70% vermiculite, N = 5). The pattern

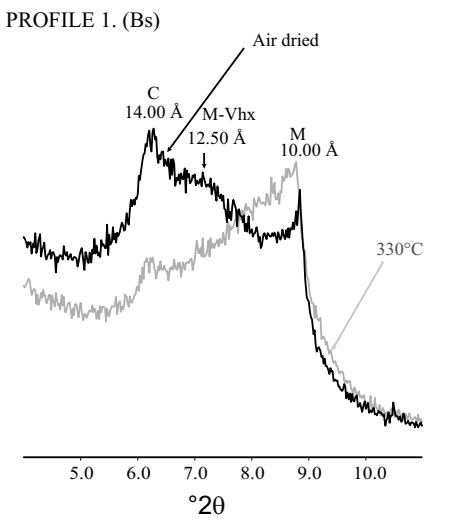

Figure 2. Profile 1(Bs): XRD patterns of the air-dried and heated at 330ºC oriented mounts of Na-saturated clay fraction. The mineral symbols are the same as for Figure 1. CuKα radiation.

of the Mg-saturated sample was significantly affected by glycerol saturation, indicating the presence of smectite. Although the fit between the calculated and measured XRD patterns was not perfect, the assumed mixture gave at least some idea of the complexity of the mineral composition of the sample analyzed.

In the XRD patterns of the random powder mounts of the clay fractions in the range 59–64º2θ, two reflections can be seen: near 1.54 Å and near 1.50 Å (Figure 4). The reflection near 1.50 Å indicates the presence of one or more dioctahedral minerals. Higher up in the profile, the intensity of the 1.50 Å reflection increases, the peak position migrates towards the greater 2θ angle and a high-angle shoulder appears. Such characteristics indicate an increase in the amount of kaolinite and Al-rich vermiculite and smectite components. The reflection near 1.54 Å may result from trioctahedral clays, but the presence of quartz makes the identification of these minerals difficult. The decrease in the 1.54 Å intensity with respect to the intensity of the 1.82 Å quartz reflection occurs up the profile indicating a decreasing amount of trioctahedral clay. A decrease in the amount of quartz up the profile is also observed. In the FTIR spectra the decrease and total disappearance of an

https://doi.org/10.1346/CCMN.2007.0550609 Published online by Cambridge University Press

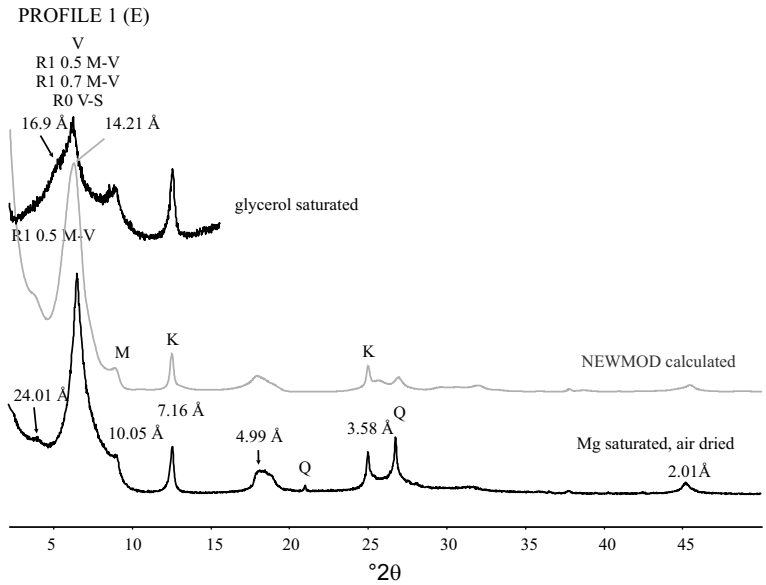

Figure 3. Profile 1(E): XRD patterns of the air-dried and glycerol-treated oriented mounts of Mg-saturated clay fraction and Newmod-calculated pattern (see the text for details). The minerals symbols are the same as for Figure 1. CuKα radiation.

absorption band at ~650 cm^{-1} is clearly observed, indicating the disappearance of trioctahedral minerals in the upper soil horizons (Figure 5).

Profile 2, Czarny Staw Lake

Mica and a mixed-layer mineral dominate the clay fraction from lower Bs/C horizon (Figure 6). The significant decrease in the intensity of the low-angle reflection after the ethylene glycol treatment suggests the presence of smectitic interlayers in the mixed-layer mineral. Partial thermal stability of the structure (after heating at 330ºC) indicates the presence of hydroxy interlayers. Chlorite, kaolinite, quartz and feldspars are also present. The clay fraction from the upper OE horizon is dominated by mica and mica-12 Å vermiculite probably without the admixture of smectite interlayers. Kaolinite and traces of quartz and feldspars are also noted. The reduced intensity of the 650 cm^{-1} absorption band observed in the FTIR spectra indicates that the fractions from both horizons are dominated by dioctahedral rather than trioctahedral species.

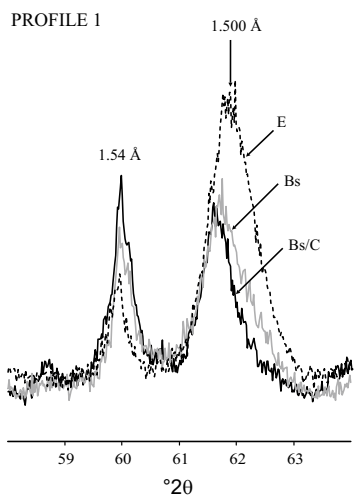

Figure 4. Profile 1: XRD patterns of random mounts of Na-saturated clay fractions. CuKα radiation.

Profile 3, Krzyżne Pass

Mica and chlorite dominate the clay fractions separated from the lower horizons (C, B/C) which also contain mixed-layer minerals with some smectite interlayers indicated by a decrease in the intensity of the 10−14 Å reflection after ethylene glycol treatment. Other minerals present are kaolinite, quartz and feldspars. The fraction from the Bs horizon contains mica, chlorite, kaolinite, quartz, feldspars and a mica-12 Å vermiculite mixed-layer mineral with a small amount of hydroxy interlayers. The Bhf horizon clay fraction consists of a smaller amount of chlorite and mica-12 Å vermiculite mixed-layer mineral without hydroxy interlayers. Mica is the most abundant mineral in the clay fraction of the E horizon (Figure 7). The fraction also contains kaolinite, mica-12 Å vermiculite, and a small amount of quartz and feldspars. The upper OE horizon contains mica, mixed-layer minerals, quartz and kaolinite (Figure 8). Most of the clay minerals seem to be dioctahedral. Traces of trioctahedral species are present only in the lower part of the profile (C and Bs/C horizons) (Figure 8).

Profile 4, Beskid Mountain

All the clay fractions are dominated by mica. They also contain kaolinite, chlorite, quartz and feldspars. A

https://doi.org/10.1346/CCMN.2007.0550609 Published online by Cambridge University Press

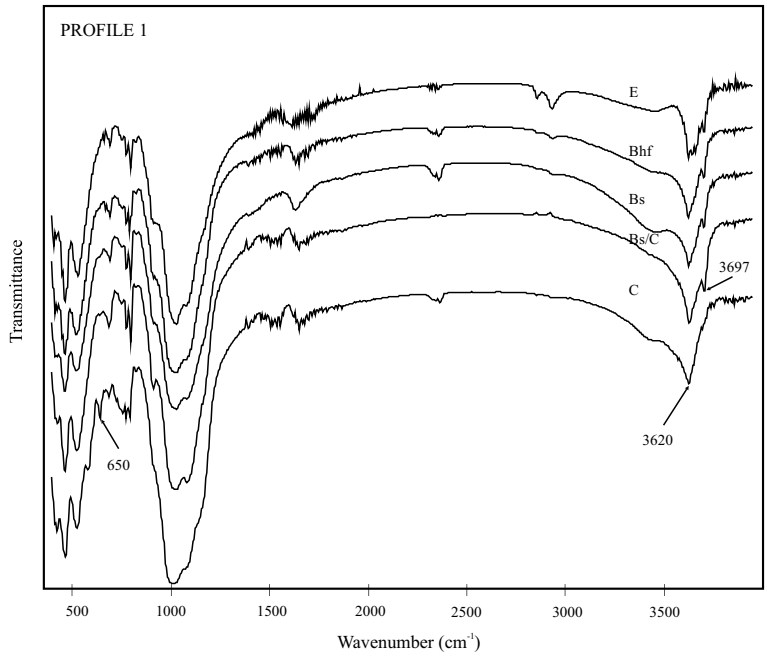

Figure 5. Profile 1: FTIR spectra of the separated clay fractions.

mixed-layer chlorite-14 Å vermiculite (C-V) was identified in all the fractions by the appearance of a reflection between 14 Å and 10 Å after heating at 550ºC (Figure 9). The C-V content decreases towards the top of the profile. Also in the clay fraction from the OE horizon, a small amount of mixed-layer minerals is present, containing smectite interlayers, as indicated by a decrease in the intensity of the 10–14 Å reflection after ethylene glycol treatment. All the fractions contain dioctahedral as well as trioctahedral clay minerals. The presence of the trioctahedral species is indicated by a strong absorption band near 650 cm^{-1} in the FTIR spectra.

Profile 5, Dolina Jarząbcza Valley

Mica (mostly dioctahedral) is the main constituent of all the fractions separated from this profile. Quartz and feldspars are also present in all the samples. The fractions from the lower horizons (C, Bs/C) also contain chlorite. In the upper horizons (Bhf and E), kaolinite,

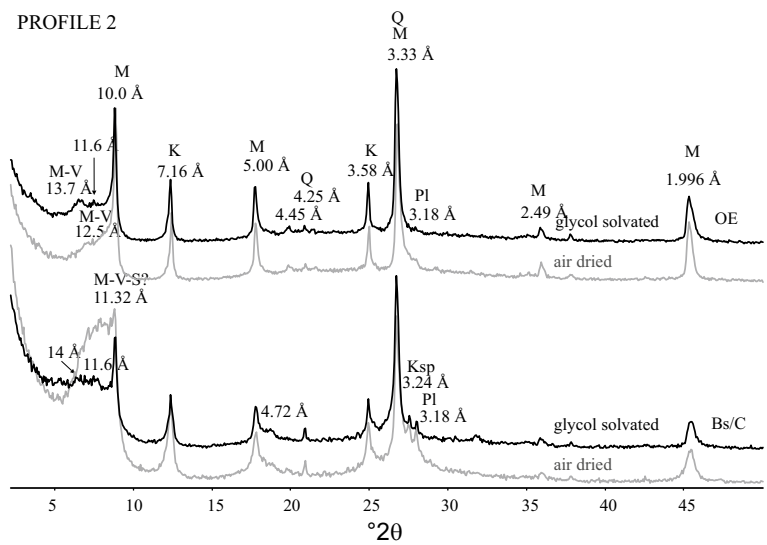

Figure 6. Profile 2: XRD patterns of the air-dried, EG-solvated oriented mounts of Na-saturated clay fractions. The mineral symbols are the same as for Figure 1. CuKα radiation.

https://doi.org/10.1346/CCMN.2007.0550609 Published online by Cambridge University Press

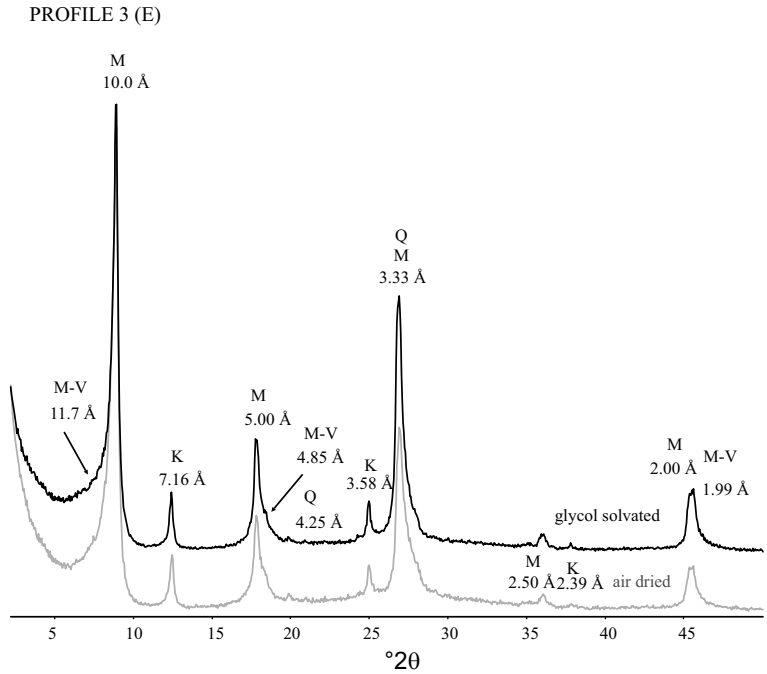

Figure 7. Profile 3(E): XRD patterns of the air-dried, EG-solvated oriented mounts of Na-saturated clay fraction. The mineral symbols are the same as for Figure 1. CuKα radiation.

and mica-12 Å vermiculite mixed-layer minerals (M-V) were identified. Some hydroxy interlayers were noted in the M-V minerals from the Bhf horizon as indicated by an incomplete shift of the 001 reflection to 10 Å after heating at 330ºC. The clay fraction from the E horizon probably contains two types of mixed-layer minerals: R0 mica-vermiculite with a large vermiculite content, and an ordered R1 M-V as indicated by the superstructure reflection appearing after ethylene glycol treatment (Figure 10). In FTIR spectra, an increase in the amount of kaolinite up the profile can be seen from the band near 3697 cm^{-1} (Figure 11).

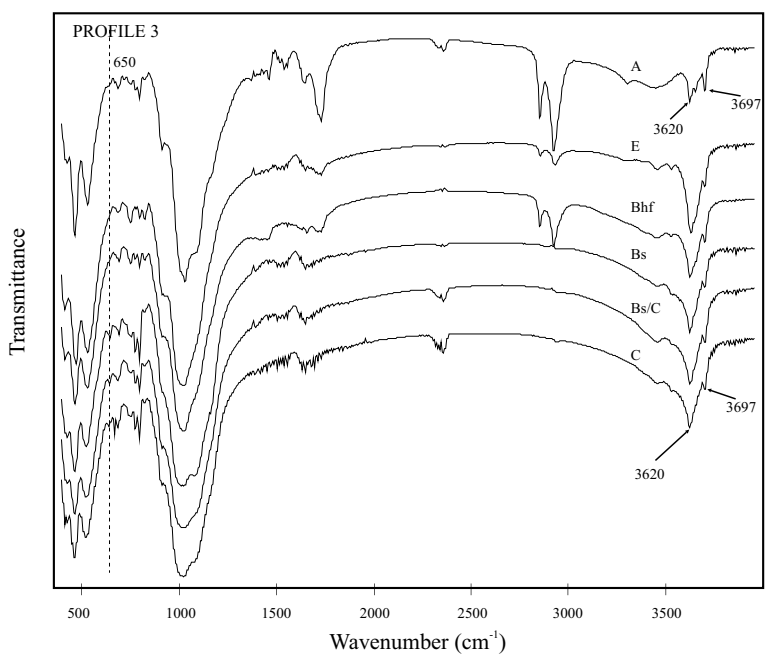

Figure 8. Profile 3: FTIR spectra of the separated clay fractions.

https://doi.org/10.1346/CCMN.2007.0550609 Published online by Cambridge University Press

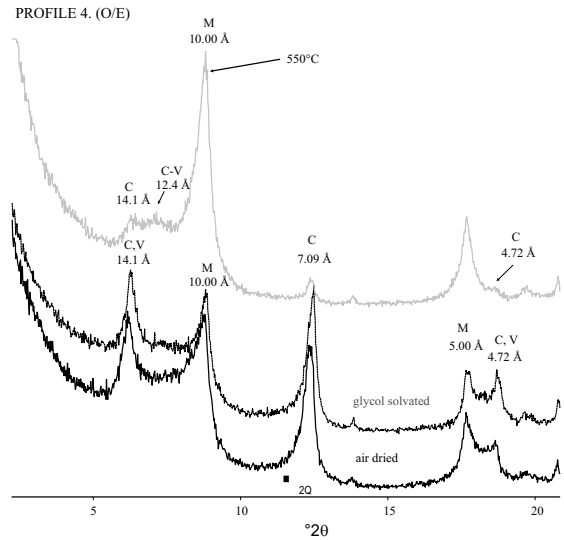

Figure 9. Profile 4(Bs/C): XRD patterns of the air-dried, and heated at 330ºC and 550ºC oriented mounts of Na-saturated clay fraction. CuKα radiation.

Profile 6, Trzydniowiański Wierch Mountain – the slope

The main constituents of the clay fractions are mica and mixed-layer minerals with swelling interlayers. Kaolinite is quite abundant in all the soil horizons while chlorite is present only in the lower part of the profile (Bs/C and Bhf horizons). Traces of quartz and feldspars are detectable in all the separated fractions, but decrease towards the top E horizon (Figure 12).

Mixed-layer minerals present in the lowest Bs/C horizon are mica-14 Å vermiculite (reflection between 10 and 14 Å remaining after glycol treatment) and mica-smectite (reflection at ~17 Å after glycol treatment). The Bhf horizon contains mica-12 Å vermiculite mixed-layer minerals with hydroxy interlayers, as indicated by partial thermal stability of the clay at 330ºC and a weak tendency to order as indicated by a superstructure reflection near 24 Å after ethylene-glycol treatment (Figure 12). The E horizon contains ordered R1 mica-12 Å vermiculite without hydroxy interlayers. The presence of R1 ordering is manifested by an almost rational series of sharp reflections, including a superstructure reflection (Figure 12). In the air-dried Na-form they correspond to 10 Å + 12.5 Å values and in glycolated Na-form to 10 Å + 13.9 Å, as well as in air-dried Mg-form, to 10 Å + 14 Å values. The XRD pattern of a Mg-saturated sample was modeled (Figure 13) using NEWMOD (Reynolds, 1985) and the best fit between calculated and measured XRD patterns was obtained for a mixture of dioctahedral mica-vermiculite mixed-layer mineral (R1, 50% vermiculite, $N = 5$) with dioctahedral vermiculite ($N = 5$) mica ($N = 20$), and kaolinite ($N = 29$). The XRD pattern of the Mg-saturated sample was not affected by glycerol saturation, indicating a lack of smectite and smectite interlayers in the sample studied.

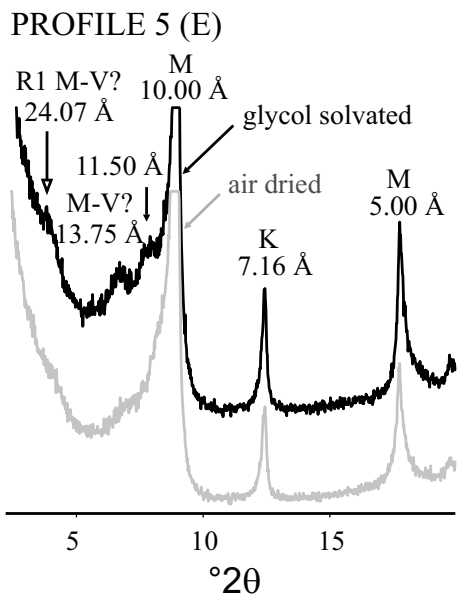

Figure 10. Profile 5 (E): XRD patterns of the air-dried, and EG-solvated oriented mounts of Na-saturated clay fraction. The mineral symbols are the same as for Figure 1.

The amount of Al-rich dioctahedral clays (kaolinite and Al-rich vermiculite) increases towards the top of the profile (Figure 14). As for profile 1, identification of trioctahedral clays was difficult.

Profile 7, Trzydniowiański Wierch Mountain – the peak

Mica and expandable clay minerals are abundant in the clay fraction of this profile. Kaolinite as well as quartz and feldspars are present in smaller amounts. Mica and kaolinite are present in all the horizons. Quartz and feldspars are also present in all the horizons and decrease up profile. The lower C and Bs/C horizons

https://doi.org/10.1346/CCMN.2007.0550609 Published online by Cambridge University Press

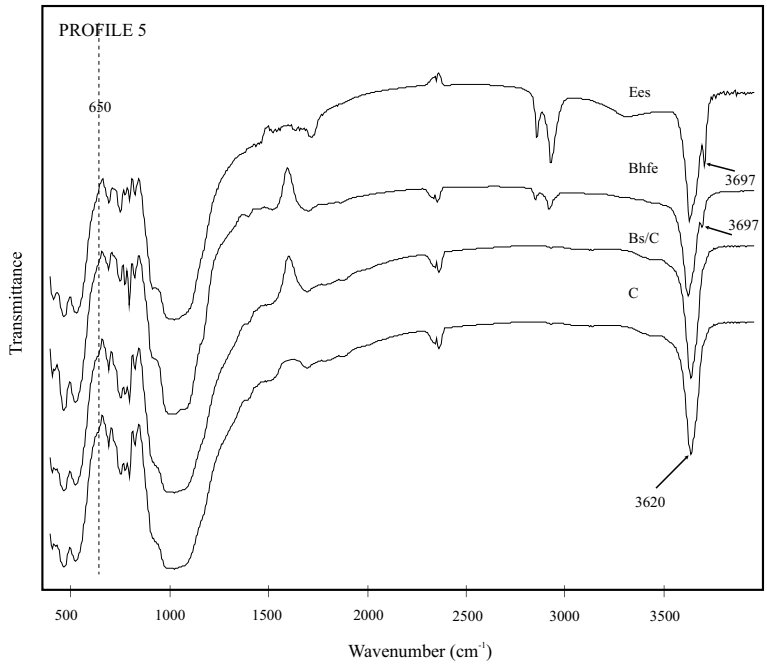

Figure 11. Profile 5: FTIR spectra of the separated clay fractions.

contain almost pure smectite (Figure 15). The Bhf horizon contains only a small amount of mica-12 Å vermiculite mixed-layer clay and probably pure 14 Å-vermiculite with some hydroxy interlayers. A partly ordered (R = 1, >50% mica) mica-12 Å vermiculite mixed-layer mineral occurs in the E horizon.

SEM images

Most of the clay particles from the lower parts of the soil profiles (C, B/C, B horizons) exhibit platy morphology with slightly rounded edges. Chemical compositions of grains indicate the presence of both dioctahedral (Al-rich) and trioctahedral (Mg-rich) layer

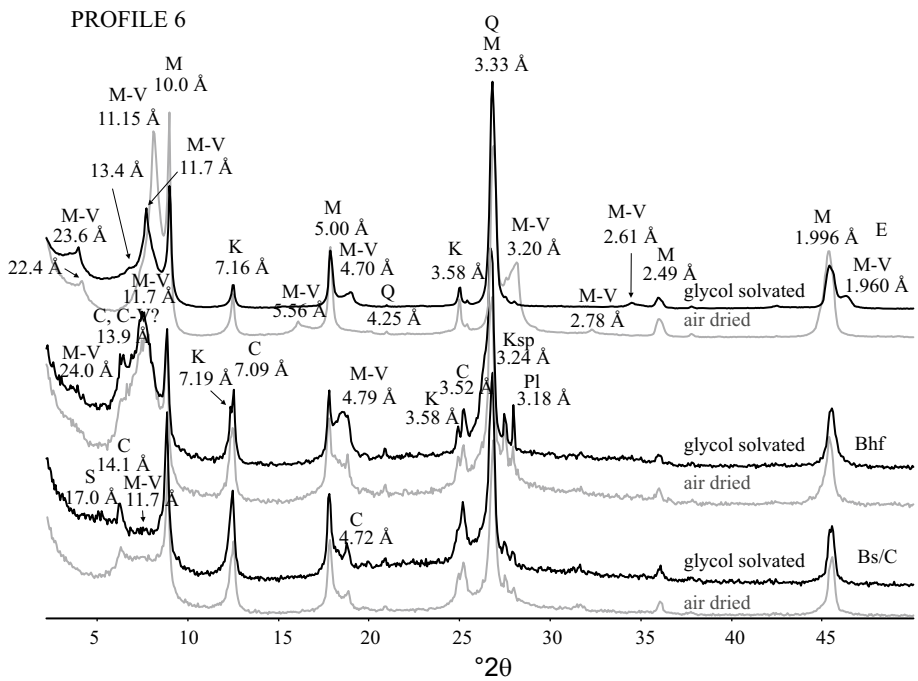

Figure 12. Profile 6: XRD patterns of the air-dried, EG-solvated, and heated at 550ºC oriented mounts of Na-saturated clay fractions. The mineral symbols are the same as for Figure 1. CuKα radiation.

https://doi.org/10.1346/CCMN.2007.0550609 Published online by Cambridge University Press

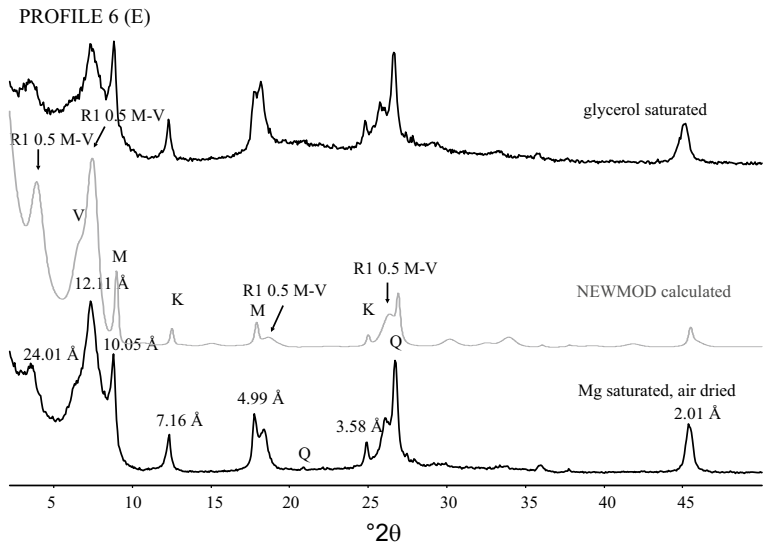

Figure 13. Profile 6(E): XRD patterns of the air-dried and glycerol-treated oriented mounts of Mg-saturated clay fraction and the Newmod-calculated pattern (see the text for details) The minerals symbols are the same as for Figure 1. CuKα radiation.

aluminosilicates. Quartz and feldspar grains are observed also. Numerous corrosion gulfs and voids, probably resulting from dissolution, are observed on the platy grain surfaces in the albic horizons (Figure 16). Most of the platy grains from this horizon contain different amounts of K, and most are rich in Al. Many of the platy grains are too thin for EDS analysis. On the surfaces of feldspars from the E horizons, numerous dissolution pits are also observed (Figure 17). In the samples from the upper soil horizons (OE, A, E), grains with hexagonal morphology were commonly noted (Figure 18). Their chemical composition indicates kaolinite.

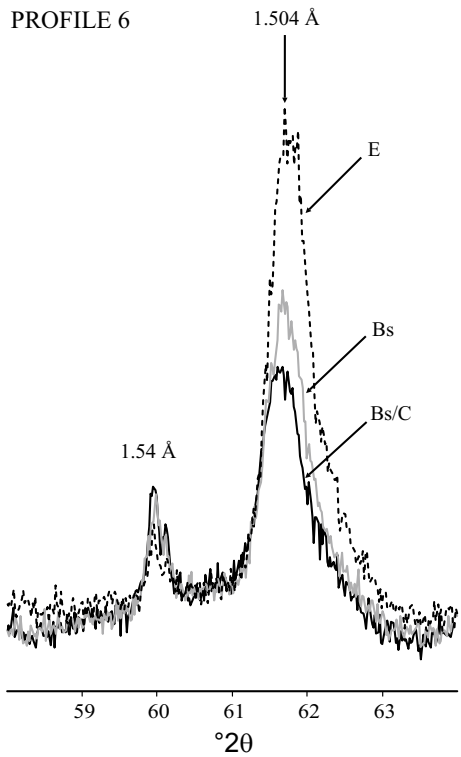

Figure 14. Profile 6: XRD patterns of random mounts of Na-saturated clay fractions. CuKα radiation.

Thin-section observations

All the platy aluminosilicate particles observed in thin-sections are strongly cracked. The cracks are parallel, perpendicular or at some angle to the aluminosilicate basal (001) planes (Figure 19). In the C, Bs/C, and B horizons, quartz, sericitized feldspars, dark mica (biotite), chlorite and light mica were identified. Chlorite/biotite intergrowths are commonly noted with the petrographic microscope and in backscattered electron images. In thin-sections, a bright mica-like mineral is the only layer aluminosilicate present in the OE and E horizons. The Al and Si contents in this light mica-like mineral are generally close to those of muscovite, but K is very variable. In the B horizons, some biotite shows K depletion along cleavage cracks suggesting transformation to vermiculite.

INTERPRETATION

When considering the origin of clay minerals in the soils studied, several processes have to be taken into account: eolian deposition, inheritance from the parent rock, dissolution of the minerals, transformation of inherited layer silicates, and neoformation of minerals during the soil process.

Eolian deposition

The process of eolian deposition in the Western Carpathians is well documented. A few spectacular

https://doi.org/10.1346/CCMN.2007.0550609 Published online by Cambridge University Press

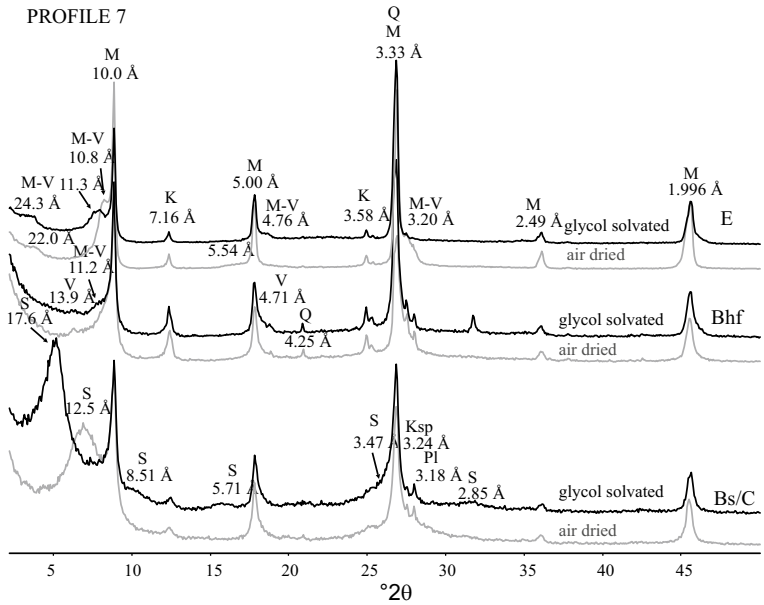

Figure 15. Profile 7: XRD patterns of the air-dried, and EG-solvated oriented mounts of Na-saturated clay fractions. The mineral symbols are the same as for Figure 1. CuKα radiation.

depositional events have been reported since the 19th century (Manecki *et al.*, 1978 and literature cited therein). The mineral composition of the dust is variable, but according to the available data, quartz seems to be the dominant mineral. Quartz, micas and probably kaolinite are the major minerals of the clay (<2 μm) fraction (Manecki *et al.*, 1978 and literature cited therein; Šucha *et al.*, 2001). If eolian input is significant in the study area, an increase in the amount of quartz, mica and kaolinite in the upper soil horizons should be observed. Kaolinite and mica do not produce clear trends in the soil profiles, although the lack of kaolinite in the lowest horizons of the profiles 1 and 5 may suggest an eolian origin. On the other hand, the upper horizons of almost all the studied profiles show a relative decrease in the amount of quartz in the clay fraction. So it can be concluded that the eolian input of clay particles is not significant, and that most of the kaolinite and mica present in the soils is not of eolian origin. One may argue that the expected distribution of the eolian clay particles (quartz, mica and kaolinite) within the profiles is disturbed by other soil processes (*i.e.* quartz dissolution and mica transformation) but no indications of quartz dissolution (*e.g.* dissolution patterns) were observed using SEM. The selective migration of quartz particles down the profile is also unlikely.

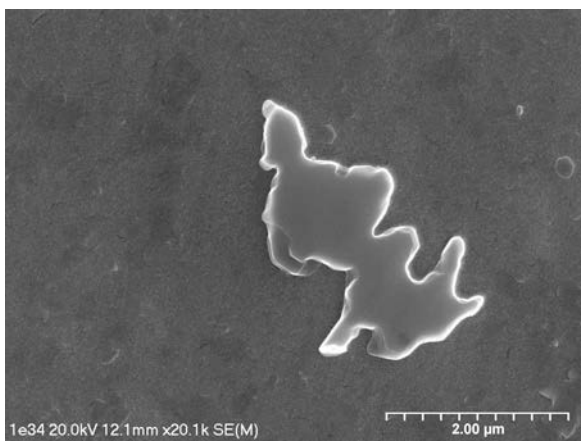

Figure 16. Corrosion gulfs developed in a dioctahedral mica grain from the albic horizon of profile 1; secondary electron (SE) image.

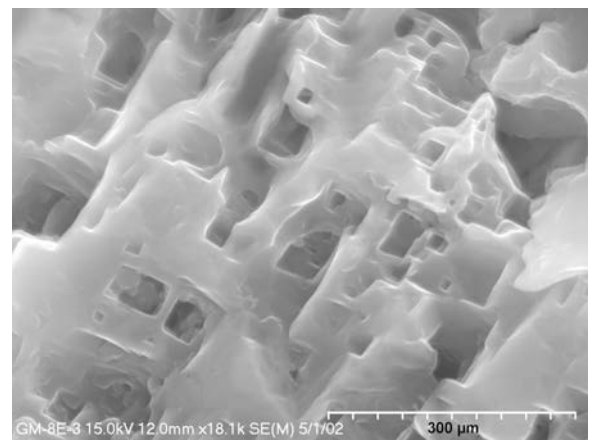

Figure 17. Dissolution patterns on a weathered feldspar grain from the albic horizon of profile 1, SE image.

https://doi.org/10.1346/CCMN.2007.0550609 Published online by Cambridge University Press

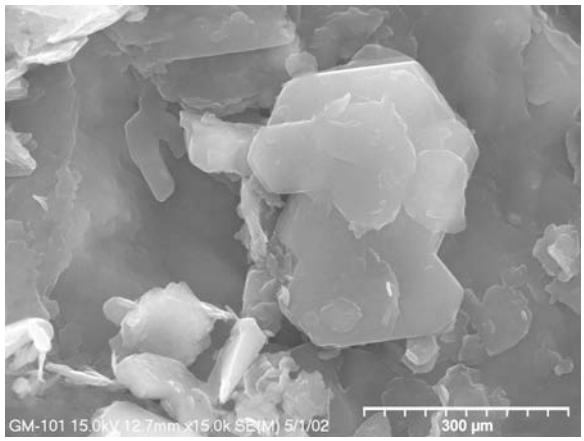

Figure 18. Hexagonal kaolinite crystal from the albic horizon of profile 1; SE image.

Inheritance from the parent material

The inheritance of clay fraction constituents from the parent rocks of the studied soils is obvious and seems to result from processes such as physical weathering of large particles (Figure 19), and the disintegration and dissolution of sericitized feldspar. In the soils studied, most of the quartz, micas, chlorite and feldspars was inherited from the bedrock. Some clay minerals may have been inherited from the previously formed (before podzolization had started) weathering crusts. It is widely accepted that the crystalline rocks in the area were subjected to strong chemical weathering during the Miocene when the climate was warm and humid (*e.g.* Klimaszewski, 1988; Passendorfer, 1971) although no such crusts have been observed, to the author's knowledge. The most likely clay mineral having such an origin is kaolinite, which is common in the studied soils. Its absence in the C horizons of the profiles 1 and 5, however, seems to exclude this possibility. Also, smectite from the C horizon of profile 7 may be the product of previous weathering, but it could also have been formed by a hydrothermal smectitization which seems to be common in the shear zones developed within the crystalline rocks in the Tatra Mountains (M. Skiba, unpublished data, 2004). Mixed-layer minerals, which contain smectite interlayers (probably R0 mica-smectite) were present in the lowest horizons of the profiles 3, 2 and 6 and could have been formed during previous weathering during the latest ice age. A 2 m thick Pleistocene weathering crust formed in permafrost conditions is the parent material for profile 3 (Oleksynowa and Skiba, 1976). It is also possible that the minerals mentioned have been derived more recently from the transformation of trioctahedral mica in the lowest horizons where the weathering has not been intensive and has affected only biotite. Such a hypothesis is consistent with the XRD and FTIR results which indicate the presence of trioctahedral species only in the lowest parts of almost all the profiles except for profile 4 in which R0 mica-smectite minerals are present in the uppermost horizon.

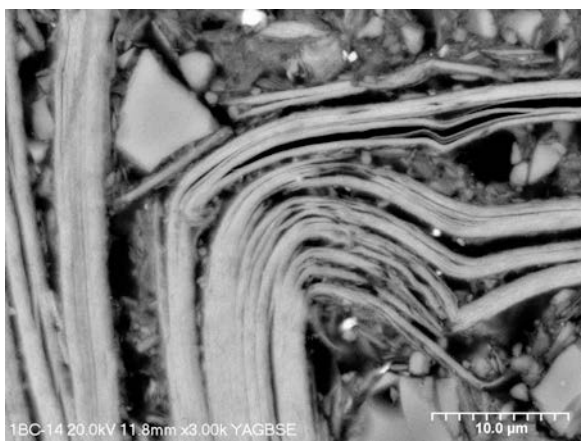

Figure 19. Disintegration of larger phyllosilicate grain from profile 1; back-scattered electron image.

Dissolution vs. dilution of non-clay minerals

A relative decrease up profile in the amount of quartz in the clay fractions is observed. This may suggest that quartz is undergoing dissolution in upper horizons. But this may simply be a relative change caused by increased amounts of clay minerals (*e.g.* inherited or neoformed). Because no dissolution patterns are observed on quartz grains using the SEM-EDS technique, it can be concluded that dilution causes the relative depletion of quartz in the clay fraction. The same trend (decrease up profile) can be observed for feldspars in all the profiles, except for profile 5. Numerous dissolution patterns observed by SEM on the surfaces of feldspar grains (Figure 17) indicate that feldspar dissolution is common.

Dissolution vs. transformation of clay minerals

The process of transformation of dioctahedral mica in the podzols has been studied in detail because of the relatively large amount of dioctahedral mica in the parent rocks. At the initial stage of weathering, which takes place in the lower soil horizons (Bs/C mainly) dioctahedral mica seems to alter into a very heterogenous material containing mica-12 Å vermiculite and probably mica-14 Å vermiculite mixed-layer minerals with different ratios of both mica and vermiculite interlayers. The products of this stage of weathering of dioctahedral mica are present, *e.g.* in the C and B/C horizons of profiles 1 and 6, in the E horizon of profile 3, and in the Bhf horizon of profile 7. With increasing intensity of weathering, the mixed-layer minerals evolve into more vermiculitic species, and if the conditions are adequate in the B horizons, hydroxide (probably Al hydroxide) polymers are deposited within the vermiculite interlayers, and mica-hydroxy-interlayered 14 Å vermiculite minerals are formed.

https://doi.org/10.1346/CCMN.2007.0550609 Published online by Cambridge University Press

Only small amounts of hydroxy-interlayers are identified in the studied soils in the spodic horizon of profiles 1, 3, 6 and 7. In all the horizons containing hydroxy-interlayered minerals, soil pH values are equal to or >4.4, while in the B horizons of the other soils in which vermiculite and smectite interlayers are identified, the pH is <4.4 (Skiba and Skiba, 2005). This suggests that in the soils studied, the formation of hydroxy interlayers is pH dependent. They seem to form when the soil pH is $\geqslant$4.4. The observed hydroxy-interlayers were probably formed by the deposition of Al-hydroxy polymers in the interlayer space of dioctahedral vermiculite, a common process (*e.g.* Wilson, 1999). But the only evidence for this is that there is no increase in the intensity of the 650 cm^{-1} band in the FTIR spectra. Further evolution of mica-vermiculite minerals towards 12 Å vermiculite can be observed in the albic horizons of profiles 1, 6 and 7. The presence of R1 mica-vermiculite minerals in the profiles indicates that the transformation proceeds *via* intermediate ordered (R = 1) or even a regular dioctahedral mica-vermiculite phase. The abundance of smectite interlayers in mixed-layer minerals from the albic horizon of profile 1 suggests that the most stable product of dioctahedral mica transformation in the studied soil is dioctahedral smectite which is formed at the expense of 12 Å dioctahedral vermiculite. In addition to the transformation described above, dissolution of dioctahedral mica particles is indicated by the presence of corrosion gulfs and dissolution voids observed on mica grains using SEM-EDS techniques.

According to the XRD data, not much can be deduced about the behavior of trioctahedral phyllosilicates during soil weathering because of their relatively small abundance in the soils under study. Chlorite present in profile 1 seems to be transformed directly into 14 Å vermiculite without the formation of an intermediate chlorite-vermiculite mixed-layer mineral. However, in profile 4, the formation of a chlorite-14 Å vermiculite mixed-layer mineral occurs. The decrease in the chlorite basal 001 reflection intensity up the profile as well as its total disappearance in albic horizon of profiles 2, 3, 5 and 6 may suggest chlorite dissolution. The different chlorite behavior might be controlled by the mineral chemistry. The problem of chlorite and biotite transformation path recognition is made more difficult by the fact that podzol profiles do not represent depth-dependent continuous weathering. Podzols have to be regarded rather as a combination of two significantly different environments, as was mentioned in the introduction. In the lower part of the profile (C, B/C and B horizons), the weathering is much less intense than in the upper albic horizon. Most of the soils studied (except for profile 4) seem to reach the state in which trioctahedral minerals from upper soil horizons have been completely dissolved. The process of dissolution of trioctahedral minerals probably occurs simultaneously with the transformation as was shown for the dioctahedral clay minerals.

Mica-smectite and smectite minerals present in the lowest parts of profiles 2, 3 and 6 disappear in the upper soil horizons. Their disappearance is probably caused by simple dissolution in a more aggressive environment. One may imagine that the minerals are formed in the upper soil horizons and illuviated down the profile, but the absence of such minerals in the lowest part of profile 1, which contains abundant smectite-rich minerals in the E horizon, excludes such a possibility.

Kaolinite is present in all the studied profiles and it does not show any clear trend. The quantity of kaolinite within all the profiles is quite similar except for profile 5, where an increase in the amount of kaolinite up the profile can be seen, and in profile 1, where there is no kaolinite in the C horizon. As was mentioned above, only a small amount of kaolinite present in the studied soil seems to be of eolian origin. Also, kaolinite originating from older weathering regimes has been ruled out. The presence of these amounts of kaolinite in the podzols might be explained by the transformation of inherited aluminosilicates or neoformation. It is more likely that the mineral is formed by the process of neoformation (crystallization from soil solutions). Such an origin is indicated by the idiomorphic hexagonal shape of its particles. The even distribution of kaolinite within almost all the profiles may indicate that the mineral crystallized from a percolating soil solution and that conditions favoring its crystallization occur in all the horizons. The concept of solution migration would explain why kaolinite is present in more or less similar quantities in all the horizons in the case of shallower soil profiles (profiles 2, 3, 4, 6, 7) and why it is absent in the lowest horizons of the profiles 1 and 5 which are relatively deeper (Skiba and Skiba, 2005). The even distribution of kaolinite may also be connected to the mineral-surface chemistry which may favor its dispersion and transport down the profile in acidic environments (*e.g.* Palomino and Santamarina, 2005).

The soils studied represent different stages of weathering induced by podzolization. These processes take place at the micro-scale and concern the clay minerals mainly. The most advanced processes occur in profile 1 and are manifested by almost total vermiculitization of dioctahedral mica and the formation of dioctahedral smectite at the expense of dioctahedral vermiculite in the uppermost horizon. The intermediate processes can be observed in profiles 2, 3, 5, 6 and 7 which contain plenty of dioctahedral mica and mica-vermiculite mixed-layer minerals in the albic horizon but do not contain any chlorite. The initial stage of weathering occurs in profile 4 where in the albic horizon there is abundant mica and a small amount of chlorite.

DISCUSSION

The influence of detrital input on the clay mineralogy of the studied soils seems to be negligible. This is based

https://doi.org/10.1346/CCMN.2007.0550609 Published online by Cambridge University Press

on the assumption that quartz is the main constituent of the eolian dusts deposited within the area, as was reported by Manecki *et al.* (1978) and Šucha *et al.* (2001), and that no significant amount of quartz is dissolved during podzolization. The assumption seems to be correct because no dissolution pits were observed on quartz grains using SEM techniques. It is widely accepted that quartz is stable in acidic environments (*e.g.* Mason, 1960); however, according to Bennett and Siegel (1987), the solubility of quartz may increase due to complexing by organic compounds.

The problem of the origin of kaolinite in podzols was widely discussed in the present author's previous work (Skiba, 2001). It was concluded that a pedogenic origin for the kaolinite present is most likely. After consideration of new data presented in this paper, especially the results of SEM observations, it seems certain that in the soils studied, crystallization of kaolinite from soil solutions (neoformation) takes place during podzolization. Crystallization of the kaolinite strongly indicates the occurrence of intense chemical weathering in the studied podzols. Kaolinite neoformation in podzols formed in temperate regions was suggested previously, *e.g.* by Gorbunov *et al.* (1963), Dixon (1989) and Weaver (1989). An intense chemical weathering which led even to gibbsite formation was described from Alpine environments (*e.g.* Reynolds, 1971; Burkins *et al.*, 1999; Righi *et al.*, 1999). According to Dixon (1989) and Weaver (1989) such intense weathering is controlled by precipitation. The evidence for kaolinite crystallization in the present paper is consistent with results from the southern hemisphere, which indicate common kaolinite formation in cold-climate conditions (Środoń, 1999, and literature cited therein).

The pH dependency of hydroxy-interlayer formation which was observed in the studied soils is very similar to that presented by Bain *et al.* (1990) in podzols from Scottish catchments. Hydroxy interlayers in the soils studied were identified after the Jackson (1969) treatment, so there is little doubt that the thermal stability of interlayers is consistent with hydroxides and not other (*i.e.* organic) types of interlayer filling. According to laboratory experiments (*e.g.* Ohashi and Nakazawa, 1996), it seems very conceivable that clay-organic complexes may have been formed in the studied soils. The formation of such complexes in soils similar to those under study (*i.e.* rich in organic matter, and acidic) was suggested previously by Theng *et al.* (1986). According to the FTIR data, it seems that the interlayering in the soils studied is of Al type. However, it is worth considering the Mg and Fe types of hydroxy interlayers which have also been described from soils (Righi *et al.*, 1993; Ghabru *et al.*, 1990).

The transformational sequence of dioctahedral mica recognized in the podzols under study is in good agreement with that presented by Righi *et al.* (1997b) who regarded dioctahedral vermiculite as a transitional phase and dioctahedral smectite of Fe-beidellite type as a stable product of dioctahedral mica weathering in podzols. However, according to XRD data, the minerals in the present study containing smectite interlayers are Al-rich without a significant amount of Fe. Similar (Al-rich) minerals were described by April *et al.* (2004). The sequence is also consistent with the data presented by Bain *et al.* (1990) who concluded that vermiculitic weathering is dominant in Scottish podzols and that vermiculitization of dioctahedral mica occurs *via* an ordered intermediate phase of R1 mica-vermiculite character. In the present paper, the almost continuous sequence of dioctahedral mica transformation (vermiculitization and formation of smectite at the expense of vermiculite) can be observed.

Chlorite present in the studied soils seems to be dissolved in some cases and in other cases it seems to be transformed into vermiculite. The exact path of the chlorite vermiculitization remains unclear. According to Wilson (1999), chlorite in podzols may undergo transformational vermiculitization or dissolution. Complete decomposition of Fe-chlorite without the formation of any new phases during podzolization was suggested, *e.g.* by Bain (1977). The formation of expandable low-charge clay minerals at the expense of chlorite in podzols from the Appenine Mountains was described in detail by Carnicelli *et al.* (1997). Also, according to Mirabella *et al.* (2002), during podzolization, chlorite can be transformed into smectite. In this paper it was concluded that in case of the dioctahedral mica the processes of dissolution and transformation occurs simultaneously. There is no reason to assume that the situation in the case of chlorite is different. The difference in the relative intensity of both processes, dissolution *vs*. transformation, may explain different chlorite behaviors.

As was mentioned above, the mica-smectite minerals, which seem to form in the lowest horizons of the studied soils, are thought to form at the expense of inherited biotite. According to Fordham (1990a, 1990b), biotite alters to a trioctahedral, illite-like mineral which is then transformed to dioctahedral vermiculite during weathering in soils. Wilson (1999) considered the process not to be very common in soil environments. At present, the mechanism of alteration of biotite in the studied podzols remains unclear.

CONCLUSIONS

(1) The eolian input to the studied soils is negligible when compared with other processes which control the mineral composition of the clay fractions. This conclusion is based on the assumption that no significant dissolution of quartz occurs in the soil environment.

(2) The process of inheritance of layer phyllosilicates from parent rocks in the studied soils is obvious and consists of the disintegration of larger grains of micas

https://doi.org/10.1346/CCMN.2007.0550609 Published online by Cambridge University Press

and chlorite, and the dissolution of feldspars which liberates significant amounts of clay-sized sericite.

(3) The decrease in the amount of quartz in the clay fractions of the studied soils observed up the profiles is caused by dilution by large amounts of inherited and neoformed clay minerals.

(4) Processes of dissolution and transformation (opening of interlayers and layer-charge reduction) occur simultaneously in the studied soils.

(5) The recognized sequence of dioctahedral mica transformation is as follows: M → R0 M-V (12 Å or 14 Å) → R0 M-12 Å V → R1 M-12 Å V → 12 Å V → V-S → S.

(6) The formation of hydroxy interlayers takes place within hydrated interlayers only, when the conditions are appropriate. It is pH dependent and starts when the pH increases above the value 4.4.

(7) In the soils studied the neoformation of kaolinite is common and the mineral crystallizes from soil solution rich in Al and Si.

ACKNOWLEDGMENTS

This study was supported by the Polish State Committee for Scientific Research (KBN) grant no. 3 P04D 026 23. The author thanks Dr Derek Bain, Dr hab. M. Michalik, Dr Per-Arne Melkerud, Prof. dr hab. Jan Środoń and an anonymous reviewer for critical reading of the manuscript and for their helpful suggestions. Prof. dr hab. S. Skiba and Dr M. Drewnik are thanked for their help with the field work. Todd Caldwell improved the English.

REFERENCES

April, R.H., Keller, D.C. and Driscoll, T. (2004) Smectite in spodosols from the Adirondack Mountains of New York. *Clay Minerals*, **39**, 99–113.

Bain, D.C. (1977) The weathering of ferruginous chlorite in a podzol from Argyllshire, Scotland. *Geoderma*, **17**, 193–208.

Bain, D.C. and Fraser, A.R. (1994) An unusually interlayered clay mineral from the eluvial horizon of a humus-iron podzol. *Clay Minerals*, **29**, 69–76.

Bain, D.C., Mellor, A. and Wilson, M.J. (1990) Nature and origin of an aluminous vermiculitic weathering product in acid soils from upland catchments in Scotland. *Clay Minerals*, **25**, 467–475.

Bednarek, R., Charzyński, P. and Pokojska, U., editors (2003) *World Reference Base for Soil Resources.* Food and Agriculture Organization of the United Nations, Polish Soil Science Society, Toruń, Poland, 106 pp.

Bennett, P. and Siegel, D.I. (1987) Increased solubility of quartz in water due to complexing by organic compounds. *Nature*, **326**, 685–686.

Brindley, G.W. and Brown, G., editors (1980) *Crystal Structures of Clay Minerals and their X-ray Identification*. Monograph **5**, Mineralogical Society, London, 495 pp.

Burkins, D.L., Blum, J.D., Brown, K., Reynolds, R.C. and Erel, Y. (1999) Chemistry and mineralogy of a granitic, glacial soil chronoseqence, Sierra Nevada Mountains, California. *Chemical Geology*, **162**, 1–14.

Carnicelli, S., Mirabella, A., Cecchini, G. and Sanesi, G. (1997) Weathering of chlorite to a low-charge expandable mineral in a spodosol on the Apennine Mountains, Italy. *Clays and Clay Minerals*, **45**, 28–41.

Dixon, J.B. (1989) Kaolin and serpentine group minerals. Pp. 467–525 in: *Minerals in Soil Environments*, 2nd edition (J.B. Dixon and S.B. Weed, editors). Soil Science Society of America, Madison, Wisconsin.

Egli, M., Mirabella, A. and Fitze, P. (2001) Clay mineral formation in soils of two different chronosequences in the Swiss Alps. *Geoderma*, **104**, 145–175.

Egli, M., Mirabella, A., Sartori, G. and Fitze, P. (2003) Weathering rates as a function of climate: results from a climosequence of Val Genova (Trentino, Italian Alps). *Geoderma*, **111**, 99–121.

Egli, M., Zanelli, R., Kahr, G., Mirabella, A. and Fitze, P. (2002) Soil evolution and development of the clay mineral assemblages of a podzol and a cambisol in 'Maggerwald', Switzerland. *Clay Minerals*, **37**, 351–366.

Farmer, V.C., Russell, J.D. and Berrow, M.L. (1980) Imogolite and proto-imogolite allophane in spodic horizons: evidence for a mobile aluminium silicate complex in podzol formation. *Journal of Soil Science*, **31**, 673–684.

Fordham, A.W. (1990a) Weathering of biotite into dioctahedral clay minerals. *Clay Minerals*, **25**, 51–63.

Fordham, A.W. (1990b) Formation of trioctahedral illite from biotite in a soil profile over granite gneiss. *Clays and Clay Minerals*, **38**, 187–195.

Ghabru, S.K., Mermut, A.R. and St. Arnaud, R.J. (1990) Isolation and characterization of an iron-rich chlorite-like mineral from soil clays. *Soil Science Society of America Journal*, **54**, 281–287.

Gillot, F., Righi, D. and Elsass, F. (2000) Pedogenic smectites in podzols from Central Finland: an analytical electron microscopy study. *Clays and Clay Minerals*, **48**, 655–664.

Gillot, F., Righi, D. and Räisänen, M.L. (2001) Layer-charge evaluation of expandable clays from chronosequence of podzols in Finland using an alkylammonium method. *Clay Minerals*, **36**, 571–584.

Gorbunov, N.I., Prusinkiewicz, Z. and Gradusow, B.P. (1963) Obrazowanije glinistych mineralow w podzolistych poćwach na piescianych porodach raznowo wozrasta. *Poćwowjedienie*, **8**, 48–57 (in Russian).

Gustafsson, J.P., Bhattacharya, P., Bain, D.C., Fraser, A.R. and McHardy, W.J. (1995) Podzolisation mechanism and the synthesis of imogolite in northern Scandinavia. *Geoderma*, **66**, 167–184.

Hoffland, E., Giesler, R., Jongmans, T. and van Breemen, N. (2002) Increasing feldspar tunneling by fungi across a north Sweden podzol chronosequence. *Ecosystems*, **5**, 11–22.

Jackson, M.L. (1969) *Soil Chemical Analysis. Advanced Course*, 2nd edition. Published by the author, Madison, Wisconsin, 895 pp.

Klimaszewski, M. (1988) *Rzeźba Tatr Polskich*. Państwowe Wydawnictwo Naukowe, Warszawa, Poland, 668 pp. (in Polish).

Kodama, H. and Brydon, J.E. (1966) Interstratified montmorillonite-mica clays from sub-soils of the Prairie Provinces, Western Canada. *Clays and Clay Minerals*, **13**, 15–173.

Konecka-Betley, K., Czępińska-Kamin&acúska, D. and Janowka, E. (1999) *Systematyka i Kartografia Gleb*. Wydawnictwo SGGW, Warszawa, Poland (in Polish).

Kubisz, J. and Oleksynowa, K. (1972) Produkty przeobrażenia minerałów krzemianowych w glebie z Krzyżnego (Tatry). *Sprawozdania z posiedzeń Komisji Naukowej Oddział PAN w Krakowie*, **16**, 530–531 (in Polish).

Lin, C.-W., Hseu, Z.-Y. and Chen, Z.-S. (2002) Clay mineralogy of Spodosols with high clay contents in the subalpine forests of Taiwan. *Clays and Clay Minerals*, **50**, 726–735.

Lundström, U.S., van Breemen, N. and Bain, D.C.(2000) The podzolisation process. A review. *Geoderma*, **94**, 91–107.

Lång, L.-O. and Stevens, R.L. (1996) Weathering variability

and aluminium interlayering: clay mineralogy of podzol profiles in till and glaciofluvial, SW Sweden. *Applied Geochemistry*, **11**, 87–92.

Madejová, J. (2003) FTIR techniques in clay minerals studies. *Vibrational Spectroscopy*, **31**, 1–10.

Manecki, A., Michalik, M., Obidowicz, A. and Wilczyńska-Michalik, W. (1978) Charakterystyka mineralogiczna i palinologiczna pyłów eolicznych z opadów w Tatrach w latach 1973 i 1974. *Prace Mineralogiczne*, **57**, 19–60 (in Polish).

Mason, B. (1960) *Principles of Geochemistry*, 2nd edition. John Wiley and Sons Inc., New York, 310 pp.

McDaniels, P.A., Falen, A.L., Tice, K.R., Graham, R.C. and Fendorf, S.E. (1995) Beidellite in E horizons of northern Idaho spodosols formed in volcanic ash. *Clays and Clay Minerals*, **43**, 525–532.

Mehra, O.P. and Jackson, M.L. (1960) Iron oxide removal from soils and clays by dithionite-citrate system buffered with sodium bicarbonate. *Clays and Clay Minerals*, *Proceedings of the 7th National Conference*, Pergamon Press, Oxford, UK, pp. 317–327.

Melkerud, P.-A., Bain, D.C., Jongmans, A.G. and Tarvainen, T. (2000) Chemical, mineralogical and morphological characterisation of three podzols developed on glacial deposits in Northern Europe. *Geoderma*, **94**, 125–148.

Michalik, M. and Uchman, A. (1998) Podłoże geologiczne Gleby. Pp. 9–35 in: *Ochrona przyrody nieożywionej i gleb, operat szczegółowy, Część I. Charakterystyka Zasobów Przyrody Nieożywione i Gleb* (S. Skiba, A. Kotarba, editors). The Tatra National Park Archives, Poland (in Polish).

Mirabella, A., Egli, M., Carnicelli, S. and Sartori, G. (2002) Influence of parent material on clay minerals formation in podzols of Trentino Italy. *Clay Minerals*, **37**, 699–707.

Mystkowski, K. (1999) ClayLab, a computer program for processing and interpretation of X-ray diffractograms of clays. Pp. 114–115 in: *Conference of European Clay Groups Association, EUROCLAY 1999. Book of abstracts*, Krakow, Poland.

Niedźwiedź, T. (1992) Climate of the Tatra Mountains. *Mountain Research and Development*, **12**, 131–146.

Ohashi, H. and Nakazawa, H. (1996) The microstructure of humic acid-montmorillonite composites. *Clay Minerals*, **31**, 347–354.

Oleksynowa, K. and Skiba, S. (1976) Geochemical characterization of a polygonal soil on the flattening of Krzyżne Pass in the Tatra Mts. *Studia Geomorphologica Carpatho-Balcanica*, **10**, 27–47.

Palomino, M.A. and Santamarina, J.C. (2005) Fabric map for kaolinite: effects of pH and ionic concentration on behavior. *Clays and Clay Minerals*, **53**, 211–223.

Passendorfer, E. (1971) *Jak powstały Tatry*, 10th edition. Wydawnictwa Geologiczne, Warszawa, Poland, 279 pp. (in Polish).

Prusinkiewicz, Z. (1994) *Leksykon Ekologiczno-gleboznawczy*. Państwowe Wydawnictwo Naukowe, Warszawa, Poland, pp. 288 (in Polish).

Reynolds, R.C. (1971) Clay mineral formation in an alpine environment. *Clays and Clay Minerals*, **19**, 361–374.

Reynolds, R.C., Jr. (1985) *NEWMOD*©, a computer Program for the Calculation of One-dimensional Diffraction Patterns of Mixed-Layered Clays. R.C. Reynolds, Jr., 8 Brook Drive, Hanover, New Hampshire, USA.

Righi, D. and Elsass, F. (1996) Characterization of soil clay minerals: decomposition of X-ray diffraction diagrams and high-resolution electron microscopy. *Clays and Clay Minerals*, **44**, 791–800.

Righi, D., Petit, S. and Bouchet, A. (1993) Characterization of hydroxy-interlayered vermiculite and illite/smectite interstratified minerals from the weathering of chlorite in a cryorthod. *Clays and Clay Minerals*, **41**, 484–495.

Righi, D., Räisänen, M.L. and Gillot, F. (1997a) Clay mineral transformations in podzolized tills in central Finland. *Clay Minerals*, **32**, 531–544.

Righi, D., Gillot, F., Elsass, F. and Petit, S. (1997b) Transformation of smectite in two contrasted soil environments. Pp. 59–61 in: *Journees Scientifiques en l'Honneur de V.A. Drits, Programme et Resumes*, Paris.

Righi, D., Huber, K. and Keller, C. (1999) Clay formation and podzol development from postglacial moraines in Switzerland. *Clay Minerals*, **34**, 319–332.

Skiba, M. (2001) The origin of kaolinite from the Tatra Mts. podzols. *Mineralogia Polonica*, **32**, 67–77.

Skiba, M. and Skiba, S. (2005) Chemical and mineralogical podzolization indicators – on the example of soils formed from granitoids. *Polish Journal of Soil Science*, **38**, 153–161.

Skiba, S. (1977) Studia nad glebami wytworzonymi w różnych piętrach klimatyczno-roślinnych krystalicznej części Tatr polskich. *Roczniki Gleboznawcze*, **27**, 205–241.

Skiba, S. (1998) Gleby. Pp. 121–147 in: *Ochrona przyrody nieożywionej i gleb, operat szczegółowy, Część I. Charakterystyka Zasobów Przyrody Nieożywionej i Gleb* (S. Skiba and A. Kotarba, editors). The Tatra National Park Archives, Poland (in Polish).

Šucha, V., Środoń, J., Clauer, N., Elsass, F., Eberl, D.D., Kraus, I. and Madejová, J. (2001) Weathering of smectite and illite-smectite under temperate climatic conditions. *Clay Minerals*, **36**, 403–419.

Środoń, J. (1999) Use of clay minerals in reconstructing geological processes: recent advances and some perspectives. *Clay Minerals*, **34**, 27–37.

Theng, B.K.G., Churchman, G.J. and Newman, R.H. (1986) The occurrence of interlayer clay-organic complexes in two New Zealand soils. *Soil Science*, **142**, 262–266.

Van Breemen, N., Lundström, U.S. and Jongmans, A.G. (2000) Do plants drive podzolization via rock-eating mycorrhizal fungi? *Geoderma*, **94**, 163–171.

Weaver, C.E. (1989) *Clays, Muds and Shales*. Developments in Sedimentology, **44**, Elsevier, Amsterdam.

Weber, J., Garcia-Gonzales, T.M. and Dradrach, A. (1998) Skład mineralogiczny bielic wytworzonych z granitów w karkonoskim piętrze subalpejskim w rejonie występowania klęski ekologicznej. *Zeszyty Problemowe Postępów Nauk Rolniczych*, **464**, 251–259 (in Polish).

Wilson, M.J. (1999) The origin and formation of clay minerals in soils: past, present and future perspectives. *Clay Minerals*, **34**, 7–25.

Wilson, M.J., Bain, D.C. and Duthie, D.M.L. (1984) The soil clays of Great Britain: II. Scotland. *Clay Minerals*, **19**, 709–735.

(*Received 21 June 2006; revised 10 July 2007; Ms. 1182*)